Front. Optoelectron. 2012, 5(1): 107–111
DOI 10.1007/s12200-012-0196-7

RESEARCH ARTICLE

Annealing effect on optical and electronic properties of silicon rich amorphous silicon-carbide films

Shuxin LI[1], Yunjun RUI[1,2], Yunqing CAO[1], Jun XU (✉)[1], Kunji CHEN[1]

1 Nanjing National Laboratory of Microstructures,
School of Electronic Science and Engineering, School of Physics, Nanjing University, Nanjing 210093, China
2 Department of Applied Physics, Nanjing University of Technology, Nanjing 210009, China

Abstract A series of Si-rich amorphous silicon carbide (a-SiC:H) thin films were deposited in conventional plasma enhanced chemical vapor deposition system with various gas ratio R = [CH_4]/[SiH_4]. The microstructural, optical and electronic properties of as-deposited films were investigated in this study. It was found that optical band gap was linearly proportional to carbon content in the films and it could be controlled in a range of 1.8–2.4 eV by changing the gas ratio, R. Both dark and photo conductivities in room temperature were decreased with the increasing of carbon content in the films, and the photosensitivity reached as high as 10^4 for the film with the optical band gap of 1.96 eV. The as-deposited samples were subsequently annealed at the temperatures of 900°C and 1000°C. The formation of nanocrystalline silicon (nc-Si) dots in amorphous silicon carbide (a-SiC) host matrix was shown. The dark conductivity was enhanced by five orders of magnitude after annealing compared with that of as-deposited films. The result of temperature-dependent conductivity suggested that the property of carrier transport was dominated by conduction process between the extended states. Furthermore, room temperature electroluminescence (EL) was achieved from nc-Si/SiC system and the possible mechanism of radiative recombination mechanism was discussed.

Keywords amorphous silicon carbide (a-SiC), optical band gap, photo-conductivity, dark conductivity, electroluminescence (EL)

1 Introducton

Nanocrystalline silicon (nc-Si) films have attracted much attention nowadays because of their novel physical properties compared with that of their bulk counterpart. When the size of nc-Si is less than the de Broglie wavelength of corresponding electrons (or holes), size-dependent properties can be observed due to the effect of quantum confined [1–3]. For example, an intense light emission invisible light region can be observed at room temperature from nc-Si films and the emission wavelength is tunable by controlling dot size. More recently, it has been proposed that nc-Si materials can be potentially used in all-Si tandem solar cells [4–6]. Since the optical band gap of nc-Si films can be controlled to match the solar spectrum and the efficiency can be improved by reducing energy loss via the process of carrier thermal relaxation. Usually, nc-Si dots are embedded in amorphous host matrix, such as SiO_2 [7]. However, the large band offset between Si and SiO_2 causes the low carrier tunneling probability, which will deteriorate the device performance. Compared to SiO_2, amorphous silicon carbide (a-SiC) materials have the low band gap, which is helpful for carrier tunneling through the barrier layers, and improve the cell efficiency [8]. Therefore, it is currently interesting to fabricate nc-Si embedded in a-SiC host matrix and study the properties of formed materials. It has been reported that by annealing the Si-rich a-SiC films at high temperature, the Si can be precipitated and the nc-Si dots are formed in SiC matrix. The Si dot size can be modulated by changing the compositions of a-SiC film and the annealing conditions [9].

In our previous work, we have studied the microstructures and optical properties of hydrogenated amorphous silicon carbon (a-SiC:H) films prepared in plasma enhanced chemical vapor deposition (PECVD) system. It was shown that the optical properties were strongly influenced by the chemical bonding configurations and film microstructures [10,11]. After annealing at 900°C, the nc-Si dots (>7 nm) can be formed and the crystallinity is

Received September 13, 2011; accepted November 15, 2011

E-mail: junxu@nju.edu.cn

about 70%. In the present work, we systematically studied the optical and electronic properties of non-stoichiometric a-SiC:H films prepared under various gas ratio of R = $[CH_4]/[SiH_4]$. In order to get small-sized Si dots (< 5 nm), we annealed the a-SiC film with different compositions and temperatures. It was found that nc-Si dots with size of around 2–3 nm could be obtained and the electronic properties were changed after annealing. Moreover, room temperature electroluminescence (EL) has been achieved from nc-Si films embedded in SiC matrix.

2 Experiments

A series of hydrogenated silicon carbon thin films were fabricated on double-polished c-Si and quartz plates in radio frequency PECVD system by using a gas mixture of silane (SiH_4) and methane (CH_4). The deposition parameters used to prepare the studied films are as follows: pressure of 10 mTorr, substrate temperature of 250°C, and power of 30 W. The gas flow rate of SiH_4 was kept at 5 sccm and the gas ratio $R = [CH_4]/[SiH_4]$ was varied from 0 to 12. After deposition, the samples were individually annealed in the conventional furnace at temperatures of 900°C, 1000°C for 1 h in nitrogen ambient.

Microstructures before and after annealing were characterized by Raman scattering spectra using a JobinYvon Horiba HR800 spectrometer operating with 1800 g/mm grating. The excitation light source is Ar^+ laser with a wavelength of 488 nm. The carbon content x in a-SiC_x:H films was evaluated by X-ray photoelectron spectra. The optical absorption of the a-Si films was measured at room temperature by Shimadzu UV-3600 spectrophotometer. The coplanar configurations by vacuum evaporation of Al electrodes on films were used to study temperature-dependent dark conductivity. The range of temperature was 300–423 K and the current was measured by using a Keithley 610 C electrometer. The photo-conductivity of the samples was also measured under an AM1.5 (100 mW/cm^2) illumination.

3 Results and discussion

Figure 1 shows the relationship between the optical band gap (E_{opt}) and the carbon content x for as-deposited a-SiC_x:H films. It is clearly shown that the optical band gap is linearly dependent with the carbon content x.The relationship can be deduced as $E_{opt}(eV) = 1.35x + 1.87$. Especially, when $x = 0$, $E_{opt} = 1.87$ eV, which is in agreement with our experimental result of the amorphous silicon. When $x = 0.36$, the optical band gap of a-SiC_x:H film is about 2.4 eV. The enlargement of band gap indicates that the weaker Si-Si bonds are gradually replaced by the stronger Si-C bonds as the carbon content increases [12]. It is worth noting the maximum carbon content in a-SiC_x:H

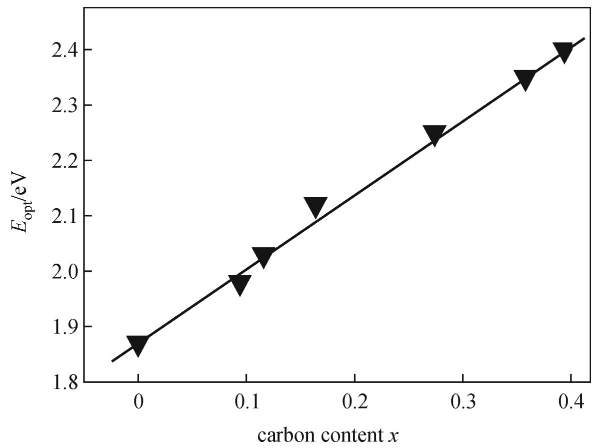

Fig. 1 Optical band gap as a function of the carbon content x for as-deposited a-SiC_x:H films

samples is $x = 0.36$, which means all the films are non-stoichiometric (Si-rich) a-SiC:H films. Figure 2 gives the absorption coefficient for different a-SiC_x:H films. It is found that the absorption coefficient is decreased with increasing the carbon content x. The absorption edge is obviously blue shifted due to the gradually increased optical band gap.The absorption coefficients become high ($>10^3$ cm^{-1}) when the wavelength exceeds the absorption edge [13].

It is interesting to study the electronic transport properties for a-SiC_x:H films with various film compositions. Figure 3 gives the room temperature dark and photo conductivities of a-SiC_x:H with different carbon content x. It is found that, with increasing the carbon content x, the dark conductivity is decreased from 10^{-8} to 6×10^{-10} S/cm due to the gradually enlargement of band gap. On the other hand, the photo-conductivity under AM1.5 illuminationis also gradually decreased from 3×10^{-4} to 6×10^{-10} S/cm with increasing the carbon content x. The decrease of photo-conductivity with increasing the carbon content x in

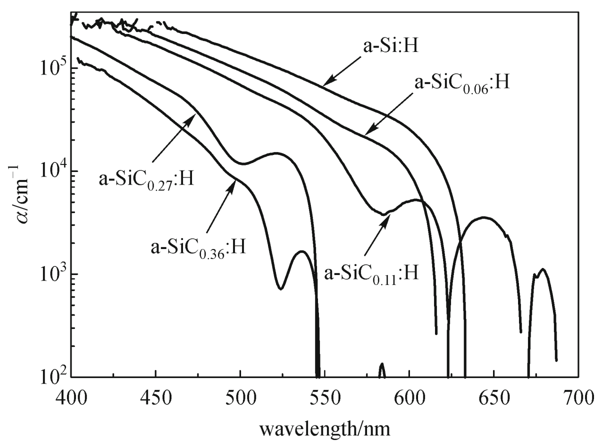

Fig. 2 Absorption coefficient spectra of as-deposited a-SiC_x:H films

films can be ascribed to the reduction of photo-excited carrier density (electrons and holes) from valence band to conduction band under the light excitation with certain photo energy. Moreover, for samples with large band gap, the fraction of solar spectrum, which can excite the electrons from valence band to conduction band, is also reduced compared to that of samples with narrow band gap. As a consequence, the photo-conductivity is gradually decreased as shown in Fig. 3. It is noted that the photo-sensitivity of a-SiC_x:H films, which is defined as the ratio of photo- conductivity to dark conductivity, is higher than 10^4 for a-SiC_x:H film with the optical band gap of 1.96 eV and it decreases to 10 for sample with optical band gap of 2.12 eV.

In order to get nc-Si dots embedded in a-SiC matrix, the films were annealed at 900°C and 1000°C, respectively. The Raman spectra of as-deposited and the annealed sample with the carbon content x of 0.27 are shown in Fig. 4. The peak centered at 480, 520 cm^{-1} represents the transverse-optical (TO) vibration mode of amorphous silicon, and the TO vibration mode of the crystallized silicon, respectively. It is shown that the crystallization occurs when the annealing temperature exceeds 900°C. From the Raman spectra, we can estimate the average size of the nanocrystalline silicon using the empirical model [14], which is about 2.0 nm for 900°C annealed film and 3.0 nm for 1000°C annealed one.

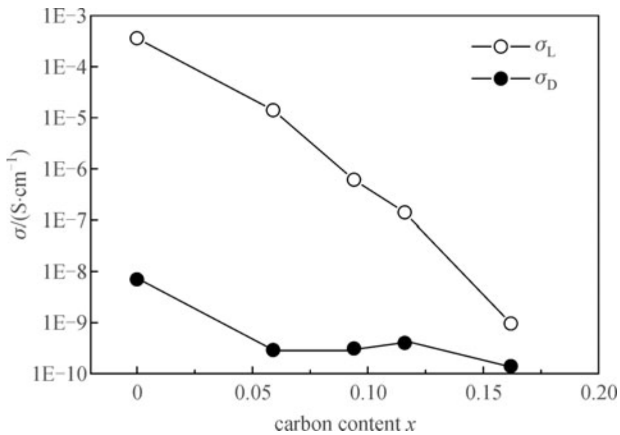

Fig. 3 Dark and photo-conductivity of as-deposited a-SiC_x:H films measured at room temperature

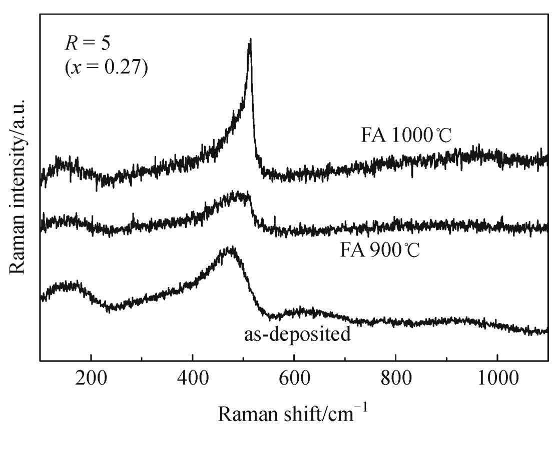

Fig. 4 Raman spectra of the sample with carbon content $x = 0.27$ before and after annealing at 900°C and 1000°C

Electronic properties were studied for annealed films and compared to that of as-deposited one in order to understand the carrier transport mechanism. Figure 5 shows the temperature-dependent conductivity (300–423 K) of the as-deposited, 900°C and 1000°C annealed samples with carbon content $x = 0.27$. The results are well agreement with the Arrhenius plots $\sigma = \sigma_0 \exp(-Ea/k_B T)$, where σ_0 is the conductivity prefactor, k_B is the Boltzmann's constant and Ea is the conductivity activation energy. It is seen that the dark conductivity exhibits the linear relationship with $1/T$ for the sample before and after annealing, which implies that the carrier transport process is controlled by the thermally activated conduction mechanism [13,15]. It is found that the room temperature dark conductivity for the 1000°C annealed films is five orders of magnitude higher than that of as-deposited film, which suggests that the existence of nc-Si dots can remarkably improve the carrier transport properties, and the corresponding conductivity activation energy is 0.53, 0.25 and 0.36 eV for the as-deposited sample and the corresponding sample annealed at 900°C and 1000°C, respectively. For the as-deposited film, the extended state conduction as usually described in the amorphous semiconductors can explain the low conductivity of the a-SiC:H films. Compared with the optical band gap (2.3 eV), the small active energy indicates that the Fermi level is shifted from the middle of the gap due to the existence of the band tail states associated with the amorphous structures. After annealing at 900°C and 1000°C, the dark conductivities are obviously increased, which can be attributed to the formation of nc-Si in the a-SiC host matrix. The crystallized Si phases, which have the

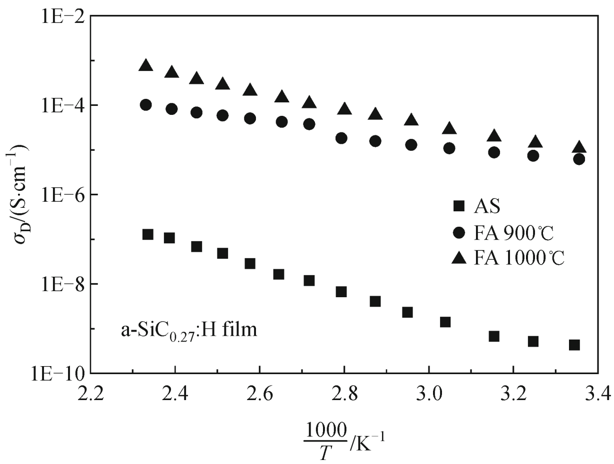

Fig. 5 Temperature-dependent dark conductivity of the as-deposited, 900°C and 1000°C annealed sample with the carbon content $x = 0.27$

small band gap compared with the a-SiC film, cause the increase of the carrier density and the enhanced mobility [16]. It is found that the optical band gap of annealed sample becomes smaller (about 2.0 eV) compared with that of as-deposited one. Consequently, the dark conductivity is significantly enhanced compared to the as-deposited film.

Room temperature EL can be observed from annealed-films [17], which cannot be detected from as-deposited samples. It is found that the film composition and annealing temperature can influence the emission peak obviously. Figure 6(a) is the EL spectra for a-$SiC_{0.27}$ film after annealing at 900°C and 1000°C, respectively. A broad EL band can be observed and peak energy is about 2.1 eV for 900°C annealed sample under injection current of 44 mA. With annealing of 1000°C, the EL peak is red-shifted to around 1.5 eV. The EL spectra were also detected for the carbon content $x = 0.16$ sample as shown in Fig. 6 (b). The EL peak energy is shifted to 1.85 eV for the carbon content $x = 0.16$ film compared to the carbon content $x = 0.27$ film after annealing at 900°C. We tentatively attributed the EL to the radiation recombination of injected electrons and holes within the nc-Si dots. The shift of EL peak energy reflects the different dot size due to the different film composition and annealing temperature. At the annealing temperature of 900°C, the size of nc-Si is smaller compared to 1000°C annealed one as we estimated from Raman spectra. Therefore, the EL peak energy is red-shifted. The film composition also influences the size of formed nc-Si after annealing. Low carbon content results in the large Si dot size after annealing, which results in the different EL peak position. The further work is undertaking to study the luminescence behaviors for annealed samples.

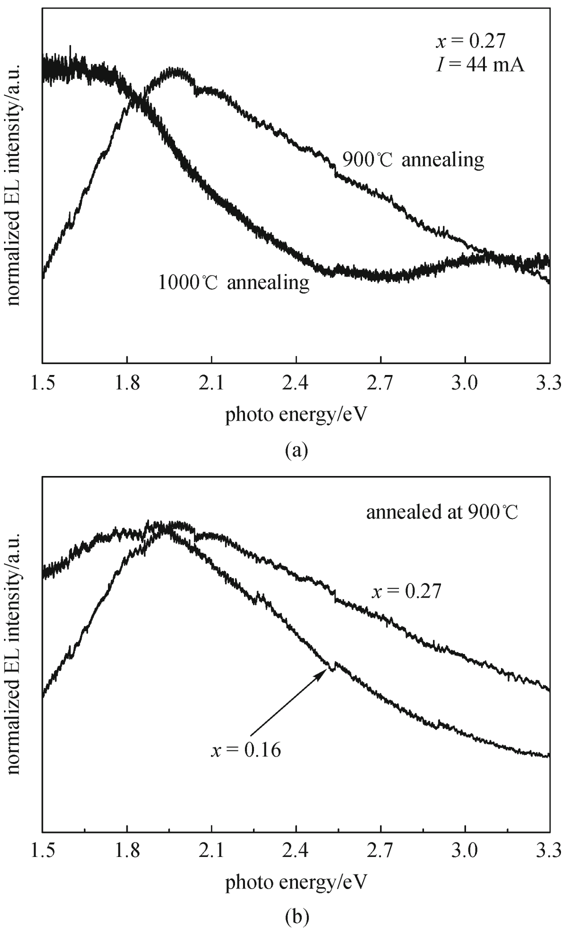

Fig. 6 (a) Room temperature EL spectra of the sample with the carbon content $x = 0.27$ after annealing at 900°C and 1000°C measured at the same injection current ($I = 44$ mA); (b) EL spectra of 900°C annealed a-$SiC_{0.27}$ film and 900°C annealed a-$SiC_{0.16}$ film

4 Conclusions

Microstructural, optical and carrier transport properties were studied for as-deposited and annealed a-SiC_x:H films with various carbon content x. With the carbon content x increases, the optical band gap changed from 1.8 to 2.4 eV for the as-deposited films, and the corresponding absorption coefficient was decreased. The photosensitivity can be as high as 10^4 for as-deposited sample with optical band gap of 1.96 eV. Annealing the films at 900°C and 1000°C caused the crystallization of Si form the nc-Si dots in a-SiC matrix as revealed by Raman spectra. The room temperature dark conductivity was five orders of magnitude higher than that of as-deposited film due to the formation of nc-Si phases. Room temperature EL was observed and the EL peak energy was shifted with the annealing temperature and film composition, which suggested that the luminescence originated from the radiation recombination of injected electron-hole pairs within nc-Si dots. Our experiment results indicated that the annealing of non-stoichiometric a-SiC_x:H films is an effective way to get small-sized nc-Si embedded in a-SiC matrix for device applications.

Acknowledgements This work was supported by National Natural Science Foundation of China (Grant No. 61036001), the National Science Foundation of Jiangsu province (No. BK2010010) and the Fundamental Research Funds for the Central Universities (No. 1112021001).

References

1. Beard M C, Knutsen K P, Yu P, Luther J M, Song Q, Metzger W K, Ellingson R J, Nozik A J. Multiple exciton generation in colloidal silicon nanocrystals. Nano Letters, 2007, 7(8): 2506–2512
2. Marsal L F, Pallares J, Correig X, Orpella A, Bardés D, Alcubilla R. Analysis of conduction mechanisms in annealed n-$Si_{1-x}C_x$:H/p-crystalline Si heterojunction diodes for different doping concentrations. Journal of Applied Physics, 1999, 85(2): 1216–1221
3. Kurokawa Y, Yamada S, Miyajima S, Yamada A, Konagai M. Effects of oxygen addition on electrical properties of silicon quantum dots/amorphous silicon carbide superlattice. Current

Applied Physics, 2010, 10(3): S435–S438

4. Song D Y, Cho E C, Conibeer G, Flynn C, Huang Y D, Green M A. Structural, electrical and photovoltaic characterization of Si nanocrystals embedded SiC matrix and Si nanocrystals/c-Si heterojunction devices. Solar Energy Materials and Solar Cells, 2008, 92(4): 474–481
5. Hanna M C, Nozik A J. Solar conversion efficiency of photovoltaic and photoelectrolysis cells with carrier multiplication absorbers. Journal of Applied Physics, 2006, 100(7): 074510–074518
6. Conibeer G, Green M, Corkish R, Cho Y, Cho E, Jiang C, Fangsuwannarak T, Pink E, Huang Y, Puzzer T. Silicon nanostructures for third generation photovoltaic solar cells. Thin Solid Films, 2006, 511-512: 654–662
7. Künle M, Kaltenbach T, Löper P, Hartel A, Janz S, Eibl O, Nickel K G. Si-rich a-SiC:H thin films: structural and optical transformations during thermal annealing. Thin Solid Films, 2010, 519(1): 151–157
8. Jiang C W, Green M A. Silicon quantum dot superlattices: modeling of energy bands, densities of states, and mobilities for silicon tandem solar cell applications. Journal of Applied Physics, 2006, 99 (11): 114902–114908
9. Solomon I, Schmidt M P, Tran-Quoc H. Selective low-power plasma decomposition of silane-methane mixtures for the preparation of methylated amorphous silicon. Physical Review B: Condensed Matter and Materials Physics, 1988, 38(14): 9895–9901
10. Xu J, Yang L, Rui Y, Mei J, Zhang X, Li W, Ma Z, Xu L, Huang X, Chen K. Photoluminescence characteristics from amorphous SiC thin films with various structures deposited at low temperature. Solid State Communications, 2005, 133(9): 565–568
11. Wang L, Xu J, Ma T, Li W, Huang X, Chen K. The influence of the growth conditions on the structural and optical properties of hydrogenated amorphous silicon carbide thin films. Journal of Alloys and Compounds, 1999, 290(1–2): 273–278
12. Harrison W A. Coulomb interactions in semiconductors and insulators. Physical Review B: Condensed Matter and Materials Physics, 1985, 31(4): 2121–2132
13. Song C, Chen G R, Xu J, Wang T, Sun H C, Liu Y, Li W, Ma Z Y, Xu L, Huang X F, Chen K J. Evaluation of microstructures and carrier transport behaviors during the transition process from amorphous to nanocrystalline silicon thin films. Journal of Applied Physics, 2009, 105(5): 054901–054905
14. Zi J, Buscher H, Falter C, Ludwig W, Zhang K, Xie X. Raman shifts in Si nanocrystals. Applied Physics Letters, 1996, 69(2): 200–202
15. Myong S Y, Lim K S, Konagai M. Effect of hydrogen dilution on carrier transport in hydrogenated boron-doped nanocrystalline silicon-silicon carbide alloys. Applied Physics Letters, 2006, 88 (10): 103120–103122
16. Song C, Rui Y, Wang Q, Xu J, Li W, Chen K, Zuo Y, Wang Q. Structural and electronic properties of Si nanocrystals embedded in amorphous SiC matrix. Journal of Alloys and Compounds, 2011, 509(9): 3963–3966
17. Rui Y J, Li S X, Xu J, Song C, Jiang X F, Li W, Chen K J, Wang Q M, Zuo Y H. Size-dependent electroluminescence from Si quantum dots embedded in amorphous SiC matrix. Journal of Applied Physics, 2011,110(6): 064322–064327